Science Bulletin 71 (2026) 444–457

Contents lists available at ScienceDirect

Science Bulletin

journal homepage: www.elsevier.com/locate/scib

Review

Recent advances and perspectives in proton-conducting metal–organic framework membranes

Jiangfeng Lu [a,1], Yiming Xu [a,c,1], Yongjun Chen [a], Xiaoqing Yu [a], Guane Wang [a], Hiroshi Kitagawa [b,*], Gang Xu [a,*]

[a] State Key Laboratory of Structural Chemistry, Fujian Institute of Research on the Structure of Matter, Chinese Academy of Sciences, Fuzhou 350002, China
[b] Department of Chemistry, Graduate school of science, Kyoto University, Kyoto 606-8502, Japan
[c] School of Physical Science and Technology, ShanghaiTech University, Shanghai 201210, China

ARTICLE INFO

Article history:
Received 23 September 2025
Received in revised form 8 November 2025
Accepted 1 December 2025
Available online 8 December 2025

Keywords:
Metal–organic frameworks
Membrane
Proton-conducting
Conduction mechanism
Fabrication approach
Protonic device

ABSTRACT

Metal–organic frameworks (MOFs), owing to their tunable pore environments and abundant hydrogen-bonding sites that enable the formation of continuous transport pathways, are widely regarded as promising candidates for proton-conducting material. Despite extensive research, most efforts have been devoted to bulk forms, such as powders and single crystals, which are hindered by long diffusion pathways, random orientation, and limited processability, thereby restricting their intergration into device. Recent progress in fabricating high-quality MOF membranes has addressed these challenges, while preserving high proton conductivity. Although notable progress has been achieved, a systematic review of proton-conducting MOF membranes remains absent. In this review, we present a comprehensive overview of proton-conducting MOF membranes, encompassing design strategies, conduction mechanisms, systematic classification, representative fabrication approaches, and their application. Particular emphasis is given to their broader application landscape, extending beyond proton exchange membrane fuel cells to include light-controlled protonic devices, proton sensors, protonic field-effect transistors, and proton rectifiers. By consolidating advances and outlining remaining challenges, this review aims to clarify design principles and guide future research toward integrating MOF membranes into next-generation protonic technologies.

1. Introduction

Metal–organic frameworks (MOFs) [1–3], also known as porous coordination polymers (PCPs) [4–6], are crystalline materials formed by the self-assembly of metal ions or clusters with organic ligands. Their highly ordered network structures endow them with key features such as high crystallinity, tunable porosity, and well-defined internal channels. Through rational selection of metal nodes, organic ligands, and their coordination modes, MOFs can be tailored with customized structures and functions, supporting their wide applicability in catalysis [7–11], sensing [12–15], gas storage [16–20], and molecular separation [21–24]. Notably, their tunable pore environments, abundant hydrogen-bonding sites, and ability to form continuous and ordered proton transport pathways make MOFs particularly well-suited for proton-conducting applications [25–27]. Specifically, incorporation of proton carriers such as water or phosphoric acid into MOF pores facilitates the formation of extended hydrogen-bonded networks, enabling efficient proton migration via both Grotthuss and vehicle mechanisms. These characteristics open new possibilities in advanced protonic devices, including proton exchange membrane fuel cells (PEMFCs) [28–31], protonic field-effect transistors (H^+-FETs) [32,33], hydrogen sensors [34–36], and proton separation technologies [37,38].

Research into MOFs as proton conductors can be traced back to 1979, when Kanda et al. [39] reported proton conductivity in a two-dimensional (2D) $(HOC_2H_4)_2$-dtoa-H_2 structure. This pioneering work laid the foundation for exploring crystalline porous frameworks as solid-state proton conductors. Over the following decades, advances in MOFs have enabled the precise design of frameworks with optimized pore environments, tailored hydrogen-bonding networks, and controllable guest incorporation,

* Corresponding authors.
E-mail addresses: kitagawa@kuchem.kyoto-u.ac.jp (H. Kitagawa), gxu@fjirsm.ac.cn (G. Xu).
[1] These authors contributed equally to this work.

https://doi.org/10.1016/j.scib.2025.12.009
2095-9273/

leading to remarkable performance improvements. In the past decade, several MOFs have achieved proton conductivities exceeding 0.1 S cm^{-1} [40–42], placing them among the best-performing solid-state proton conductors. These achievements have firmly established MOFs as a versatile and high-performance platform for proton conduction, stimulating efforts to adapt them into more application-oriented material formats.

Early studies on proton-conducting MOFs primarily focused on bulk forms such as powders or single crystals [43–47]. While valuable for fundamental studies, these formats are often unsuitable for practical integration into devices due to poor mechanical stability, uncontrolled crystal orientation, and inefficient interfacial contact. The fabrication of MOF membranes has been investigated since the early 21st century [48], offering a promising route to overcome these challenges. However, their potential for proton conduction was not widely recognized until 2013 [49], largely due to difficulties in achieving dense, continuous, and well-ordered membranes—qualities that are critical for efficient proton transport. Well-structured MOF membranes provide multiple advantages, including controlled pore orientation, reduced transport resistance, enhanced mechanical durability, and compatibility with integrated device fabrication—all of which are essential for practical protonic applications [50,51]. As a result, research interest in proton-conducting MOF membranes has surged in recent years. Previous reviews have largely focused on MOF-based mixed-matrix membranes (MMMs) and their performance in PEMFCs. Nevertheless, an overarching review addressing proton-conducting MOF membranes as an integrated topic is still lacking, and such a comprehensive summary is urgently needed to consolidate current knowledge and accelerate further development in this field.

This review systematically summarizes recent progress in proton-conducting MOF membranes, with an emphasis on conduction mechanisms, fabrication strategies, structural classifications, and emerging device applications. It also outlines key challenges and future directions to guide continued progress in this research field.

2. Conduction mechanisms and design strategies of proton-conducting MOFs

2.1. Conduction mechanisms of proton-conducting MOFs

Proton conduction in MOFs is primarily governed by two distinct yet often coexisting mechanisms: the Grotthuss mechanism [52] and the vehicle mechanism [53] (Fig. 1). The Grotthuss mechanism, also referred as proton hopping, involves the rapid hopping of protons along a continuous hydrogen-bonded network. This pathway typically originates from the water molecules or hydrogen-bonding functional groups (e.g., -OH, $-NH_2$, $-SO_3H$) within MOF channels. In this mechanism, protons are transported between adjacent donor and acceptor sites without involving the mass transport of the molecules themselves. It is characterized by low activation energy (E_a) (typically < 0.38 eV), reflecting efficient long-range proton migration. In crystalline MOFs featuring confined, quasi-one-dimensional water clusters—such as those observed in UiO-66 [54] and MIL-53 series [55,56]—the Grotthuss mechanism often dominates under humid conditions, particularly at relative humidity (RH) levels above 60%.

In contrast, the vehicle mechanism entails the physical diffusion of protonated species—such as hydronium (H_3O^+), ammonium (NH_4^+), or imidazolium-based carriers—through the MOF pores. This diffusion-driven process typically exhibits higher activation energy (typically > 0.38 eV) and is limited by steric hindrance within the MOF framework as well as the viscosity of the carrier environment. MOFs with larger pores or hydrophobic internal surfaces, such as HKUST-1 [57] or ZIF-8 [58], often favor this mechanism, especially under low-humidity or high-temperature conditions where hydrogen-bond networks are insufficiently developed.

The prevailing conduction mechanism in a given MOF is determined by the interplay between its structural features and operating environment. Rather than being strictly exclusive, Grotthuss- and vehicle-type processes often coexist, with their relative contributions shifting according to pore hydrophilicity, connectivity of hydrogen-bond networks, humidity, and temperature. Understanding this relationship provides clear design guidelines: tailoring pore topology to promote continuous hydrogen-bond chains, introducing functional groups to increase proton donor density, confining mobile carriers without excessive steric hindrance, and exploiting framework flexibility to enable dynamic rearrangement of conduction pathways. Such strategies have yielded MOFs with proton conductivities exceeding 10^{-2} to 10^{-1} S cm^{-1} under ambient or humidified conditions [59–61].

Temperature-dependent electrochemical impedance spectroscopy (EIS) [62] is commonly employed to distinguish between conduction mechanisms, with activation energies derived from Arrhenius plots. Complementary techniques—such as quasi-elastic neutron scattering (QENS) [63], solid-state nuclear magnetic resonance (NMR) [64], and molecular dynamics (MD) simulations [65]—offer molecular-level insights into proton dynamics within the MOF channels.

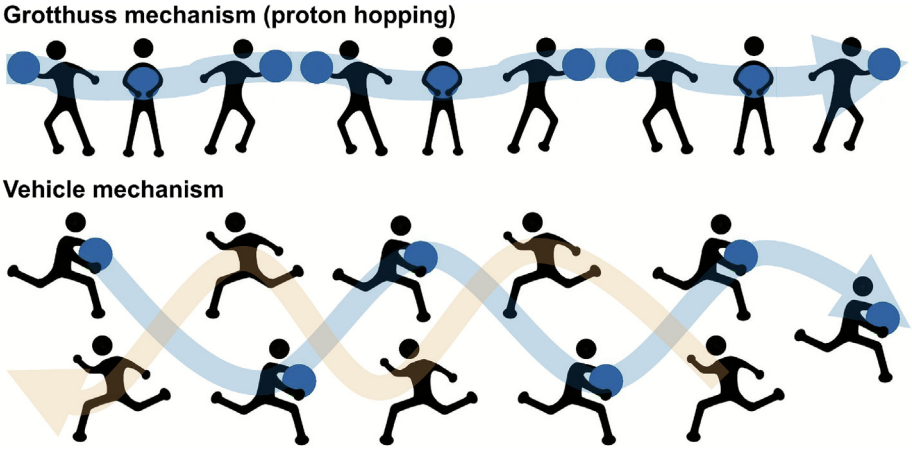

Fig. 1. Schematic illustration of the Grotthuss and vehicle mechanisms.

2.2. Design strategies of proton-conducting MOFs

Building on the structure and mechanism correlations discussed in Section 2.1, the inherent structural tunability of MOFs allows for a variety of rational design strategies aimed at enhancing proton conductivity. These approaches operate by modulating both the intrinsic framework characteristics and the local proton transport environment (Fig. 2). Five representative and interconnected strategies can be summarized as follows: (i) ligand functional group modification: incorporating hydrophilic groups such as -OH, $-NH_2$ and $-SO_3H$ into MOF ligands promotes hydrogen-bond formation, enhances water adsorption and facilitates efficient proton hopping [66]. (ii) Metal center modulation: employing high-valence or highly polarizable metal centers increases framework polarity and hydration ability, thereby promoting the generation and migration of proton carriers [67]. (iii) Defect regulation: introducing structural defects—such as deprotonated hydroxyl groups or missing linkers—can create additional proton sources or create open sites, facilitating the formation of complex hydrogen-bond networks and extra proton conducting pathways [68]. (iv) Counterion introduction: designing MOFs with charged frameworks and introducing mobile protonic counterions (e.g., H_3O^+, NH_4^+) increases the carrier concentration and supports ion-pair-based proton transport [69]. (v) Injection of functional guest molecules: doping MOF pores with acidic guest molecules (e.g., HCl, H_2SO_4) can directly supply protons and improve conductivity. However, this requires MOFs with high chemical and hydrolytic stability to prevent structural degradation [70].

Applied either individually or in synergy, these strategies enable fine-tuning of conduction pathways and precise control over the balance between Grotthuss and vehicle mechanisms. By embracing such mechanism-oriented design, researchers have realized MOFs that exhibit stable and high proton conductivity under ambient or humidified conditions. This progress not only highlights the versatility of MOFs as tunable proton conductors but also demonstrates that their practical integration into next-generation protonic devices is most effectively realized through thin-film architectures. The following section therefore summarizes representative methods for fabricating such MOF membranes.

3. Main methods for the fabrication of MOF membranes

A variety of strategies have been developed for fabricating MOF membranes to meet requirements in porosity, thickness, crystallinity, and mechanical stability. Representative approaches include *in situ* growth, layer-by-layer (LbL) assembly, electrochemical deposition, MMM, and melt-quenching methods [71]. These methods provide versatile routes to tune membrane properties and expand their applicability in functional applications, with proton conduction being one of the most actively explored directions.

In situ growth is among the most widely used strategies, relying on direct nucleation and crystallization of MOFs on substrate surfaces. This approach can be carried out under solvothermal or hydrothermal conditions (Fig. 3a), or through vapor-assisted and diffusion-limited processes. It is relatively simple and broadly applicable, typically producing membranes with strong adhesion and high crystallinity, which in turn favor ordered transport pathways. A representative example is the MOF-801 membrane, which demonstrated compact film formation with well-intergrown crystallites and uniform surface coverage, enabling efficient proton transport and reliable impedance-based sensing performance [72]. Nevertheless, precise control over thickness and large-area uniformity remains difficult, and membrane quality is strongly influenced by substrate. For proton conduction, the presence of well-defined crystalline domains facilitates directional proton transport, whereas uncontrolled growth may introduce defects or grain boundaries that increase resistance.

The LbL method involves the sequential deposition of metal ions and organic linkers, driven by electrostatic interactions, hydrogen bonding, or coordination chemistry. Typically conducted via dip coating method (Fig. 3b), this approach allows precise control of membrane thickness and orientation. Its modular nature facilitates the incorporation of functional groups and complex architectures. A limitation, however, is that the process requires careful parameter control, which may complicate scaling-up. Nevertheless, these practical challenges do not undermine its advantages for proton conduction, as LbL membranes often exhibit high orientation and tunable hydrophilicity—both of which enhance proton transport efficiency—as exemplified by the $Cu_2(F_2$-AzoBDC$)_2$(dabco) membrane [73].

Electrochemical deposition, especially anodic deposition, is a powerful technique for fabricating MOF membranes on conductive substrates under externally applied electric fields (Fig. 3c) [74]. For example, Li et al. [75] successfully grew a Zn-based MOF membrane directly on a zinc substrate via anodic deposition. In this process, ligands in the electrolyte react with metal ions oxidized near the anode, leading to direct MOF membrane growth. This approach enables rapid and mild membrane formation, facilitates localized deposition, and supports straightforward device integration, making it attractive for practical applications. However, membrane crystallinity and quality are highly sensitive to deposition parameters, and only conductive substrates can be used, which restricts the applicability of these membranes to specific device configurations. The resulting membranes typically form continuous, well-adhered frameworks with controllable thickness, providing interconnected pathways that facilitate efficient proton transport.

Compression molding and solution evaporating casting are two commonly used methods for fabricating MMMs (Fig. 3d, e). In compression molding, MOF particles are blended with a polymer matrix and then compressed into a membrane—an approach

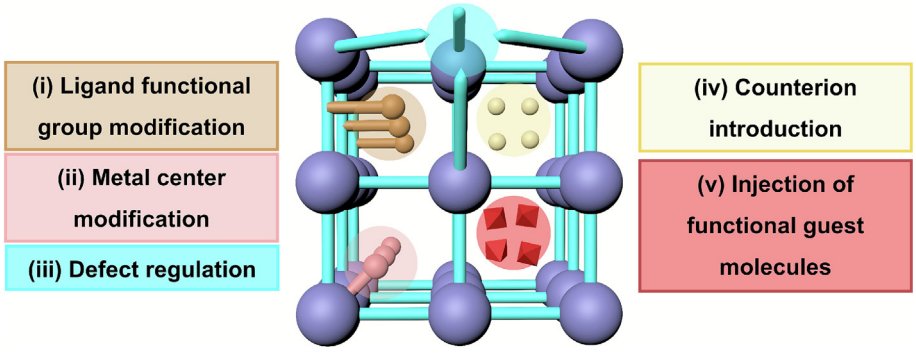

Fig. 2. Schematic illustration of design strategies for proton-conducting MOFs.

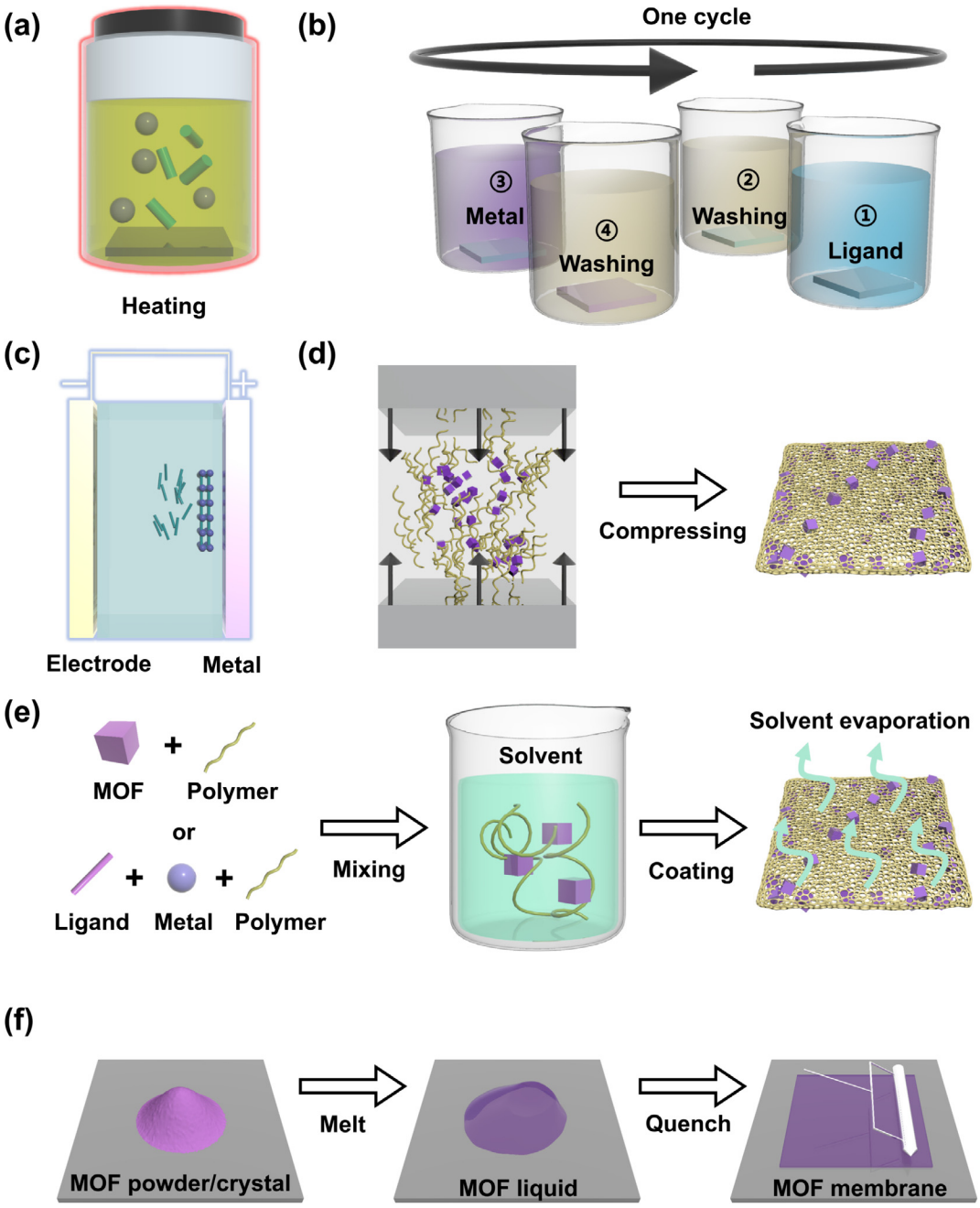

Fig. 3. Fabrication methods of proton-conducting MOF membranes. (a) Solvothermal/hydrothermal method; (b) dip coating method; (c) anodic deposition method; (d) compression molding method; (e) solution evaporating casting method; (f) melt-quenching method.

successfully implemented in the PCMOF/CNC system, where strong filler-matrix interactions contributed to enhanced mechanical integrity [76]. In solution evaporating casting, metal ions, organic linkers, and polymers are co-dissolved to allow MOFs to grow *in situ* on the polymer surface, or pre-synthesized MOF powders are dispersed with polymers in a solvent before solvent removal. A representative case is the Ni-BDC/polyacrylonitrile (PAN) membrane, in which pre-synthesized MOF particles were homogeneously dispersed within the polymer matrix through solution evaporation [77]. Both approaches are simple, broadly compatible with diverse filler-polymer combinations, and capable of producing dense, well-integrated structures with improved mechanical strength and processability. Moreover, they can accommodate high MOF loadings, and functional groups on the polymer chains may interact with MOFs to establish efficient proton conduction pathways and dense hydrogen-bonding networks. Nevertheless, both methods face similar challenges, particularly at the MOF-polymer interface, which may hinder proton transport, as well as difficulties in ensuring uniform membrane formation.

The melt-quenching method, exemplified by a_gZW-MOF·HA and $[Zn(HPO_4)(H_2PO_4)](ImH_2)_2$ membranes [78,79], involves melting crystalline MOF powders at high temperatures followed by rapid cooling to yield amorphous glassy membranes (Fig. 3f) [80,81]. These membranes are mechanically robust, largely free of grain boundaries, and can be produced over large areas, offering superior processability and stability compared with their

crystalline counterparts. The continuous, grain-boundary-free structure provides isotropic pathways that facilitate efficient proton transport. The main limitation of this approach is the loss of long-range order, which reduces porosity and may restrict ion mobility.

4. Proton-conducting MOF membranes

Since the initial report by Kanda et al. [39] in 1979 on proton conduction in MOFs, research in this area has expanded significantly. Early investigations mainly focused on single-crystal and powder forms of MOFs, which exhibited promising intrinsic proton conductivity. However, the bulk form posed inherent limitations, including long proton transport pathways, random crystal orientation, and substantial grain boundary resistance at particle interfaces, which severely hinders proton transport and, consequently, limits their practical applicability. To overcome these challenges, increasing attention has been directed toward MOF membranes, which offer advantages such as reduced transport resistance, tunable microstructures, and enhanced compatibility with device architectures—particularly for use in PEMFCs and other advanced protonic devices.

Proton-conducting MOF membranes can generally be categorized into two major types: (i) pure MOF membranes, which include both substrate-supported and self-supporting formats, and (ii) MOF-based MMMs. Pure MOF membranes offer ordered conduction pathways and intrinsic structural regularity, but their mechanical fragility and fabrication difficulty can limit scalability. In contrast, MMMs provide superior mechanical robustness and processability, yet interfacial mismatch between MOF and polymer phases may hinder proton transport. Therefore, the optimal membrane configuration should be determined based on the intended application, considering the trade-offs between conductivity, stability, and scalability. This section provides a comprehensive overview of recent progress in both types.

4.1. Pure MOF membranes

4.1.1. Substrate-supported MOF membranes

Substrate-supported MOF membranes are typically grown or transferred onto rigid or flexible substrates, enabling excellent mechanical stability and thermal resistance. These membranes benefit from highly ordered crystal orientation and shortened ion transport paths, which reduce migration resistance while maintaining the intrinsic porosity and high surface area of MOFs. Thickness and orientation can be finely tuned to optimize proton transport.

In 2012, Kitagawa's group [82] introduced a stamp-transfer strategy for fabricating highly crystalline and oriented Cu-TCPP membranes (Fig. 4a). This system employed tetracarboxylate ligand (TCPP) coordinated with Cu^{2+} to form 2D nanosheets stacked in an ABAB configuration via van der Waals interactions (Fig. 4b) [49]. The nanosheets were dispersed in ethanol, assembled at the air-water interface and transferred onto solid substrates. The resulting membranes demonstrated a dramatic conductivity enhancement—from 3.2×10^{-8} to 3.9×10^{-3} S cm^{-1} as the RH increased from 40% to 98% at 25 °C, its strong humidity-dependent conductivity originates from the Grotthuss mechanism through a hydrogen-bonded water network. This work provided early experimental evidence that MOF membranes can serve as efficient proton-conducting platforms.

Shortly thereafter, in 2014, Chao and co-workers [83] developed a mild, salt-free *in situ* growth method using copper foil as both substrate and metal source. Surface copper atoms were oxidized by dissolved oxygen to generate Cu^{2+}, which subsequently reacted with benzene-1,3,5-tricarboxylic acid (BTC) ligands to form dense HKUST-1 membranes (up to 10 × 10 cm^2 in size and several micrometers thick). Under high humidity, the membrane exhibited a proton conductivity of ~10^{-4} S cm^{-1}, significantly higher than that of HKUST-1 powder (~10^{-6} S cm^{-1}), demonstrating the clear advantage of thin-film morphology.

In 2017, Zhang et al. [84] reported a high-porosity NENU-3 membrane synthesized on copper foil via a one-step electrochemical method. By incorporating phosphotungstic acid (PTA) into the cage cavities of the $Cu_3(BTC)_2$ framework (Fig. 4c), they achieved a conductivity of 2.9×10^{-5} S cm^{-1} at 40 °C and 97% RH. The enhanced conductivity originates from a synergistic combination of the Grotthuss and vehicle mechanisms enabled by phosphotungstic acid dopants, which act as proton carriers and form extended hydrogen-bonding networks, thereby reducing the activation energy from 0.65 (pristine HKUST-1) to 0.38 eV. This work demonstrated a precise and scalable route for enhancing proton transport via guest molecule integration.

4.1.2. Self-supporting MOF membranes

Self-supporting MOF membranes—free of any substrate constraints—offer increased design flexibility, enhanced porosity, and higher surface areas, all of which are beneficial for proton transport. Owing to their standalone architecture, self-supporting membranes facilitate revealing the intrinsic properties of the materials, such as flexibility and selective separation capabilities, and allow for more versatile integration into multifunctional devices. This opens broad prospects for applications in the energy sector and the development of novel devices.

Kitagawa's group [85] has developed several crystalline self-supporting MOF membranes using vacuum filtration of exfoliated 2D nanosheets. In 2022, they reported a Cu_3TCPP membrane (Fig. 5a) prepared by the vacuum filtration method, which exhibited excellent mechanical flexibility. The proton conduction of this membrane shows obvious humidity dependence. When the RH changes from 50% to 95% the proton activity increases by five orders of magnitude. This is because the hydrogen bond network composed of water molecules and framework provides more proton conduction paths. In 2023, this approach was extended to Cu-BDC (Fig. 5b) and Cu_2Ni-TCPP membranes (Fig. 5c), showing proton conductivities of 7.2×10^{-4} and 1.3×10^{-5} S cm^{-1} at 45 °C and 98% RH, respectively [86,87]. Notably, the Cu_2Ni-TCPP membrane (8 μm thick) retained conductivity under bending with a critical curvature below 1 mm—the first demonstration of proton-conducting performance in MOF membranes under mechanical deformation—highlighting the potential of crystalline membranes for wearable and flexible devices.

Beyond crystalline nanosheet assemblies, amorphous MOF glass membranes have recently emerged as a complementary class of self-supporting proton conductors with distinct advantages in mechanical robustness. Wan and co-workers [78] developed a universal "zwitterion modification + pore acid filling + melt-quenching" strategy to vitrify highly stable carboxylate MOFs, producing a processable glass membrane (a_gZW-MOF·HA) (Fig. 5d) with an anhydrous proton conductivity of 1.57×10^{-2} S cm^{-1} at 100 °C—nearly an order of magnitude higher than its crystalline precursor. Remarkably, this membrane could partially revert to the crystalline state upon solvent stimulation, enabling a reversible "glass ↔ crystal" transformation and offering a pathway toward recyclable proton conductors. The combination of high conductivity, stability, and reprocessability positions MOF glass membranes as a valuable complement to crystalline membranes for next-generation flexible protonic technologies.

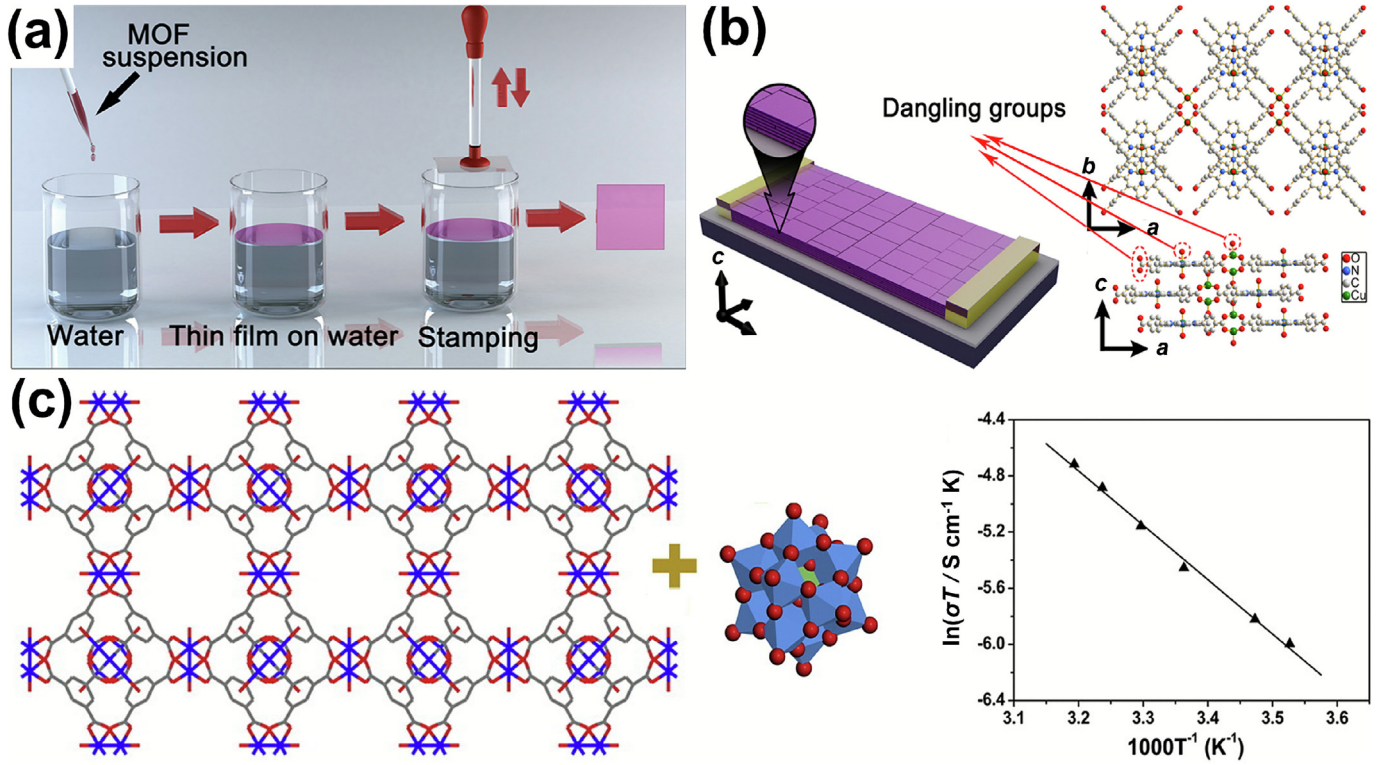

Fig. 4. Representative examples of substrate-supported MOF membranes. (a) Schematic illustration of stamp-transfer method for MOF membranes; reprinted with permission from Ref. [82], Copyright © 2012, American Chemical Society. (b) Structure and stacking mode of Cu-TCPP nanosheets; reprinted with permission from Ref. [49], Copyright © 2013, American Chemical Society. (c) Construction of high-porosity NENU-3 membranes and their proton conductivity; reprinted with permission from Ref. [83], Copyright © 2017, Elsevier B.V.

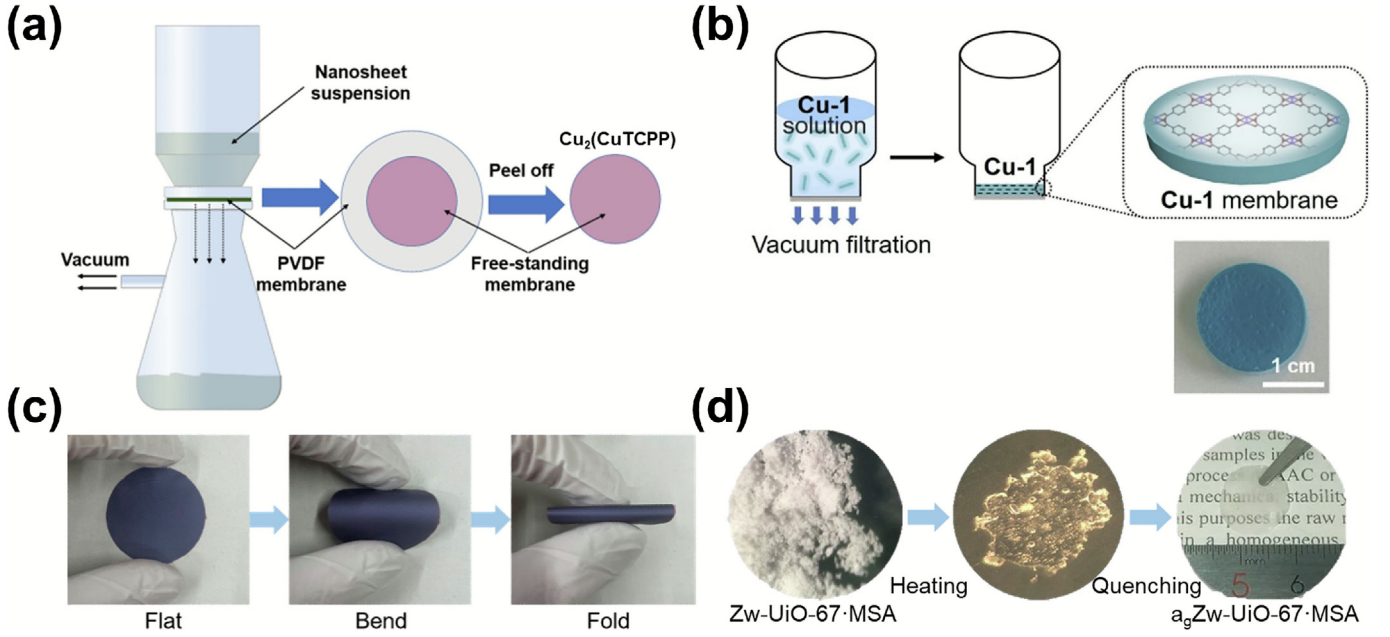

Fig. 5. Representative examples of self-supporting MOF membranes. (a) Schematic of the vacuum filtration method for preparing self-supporting MOF membranes. (b) Vacuum filtration preparation of CuBDC self-supporting membrane; reprinted with permission from Ref. [86], Copyright © 2023, Wiley-VCH. (c) Flexural performance test of Cu_2Ni-TCPP membrane (thickness 8 μm); reprinted with permission from Ref. [87], Copyright © 2023, Wiley-VCH. (d) Microscopic images of the melted, quenched, and a_gZW-UiO-67·MSA glass sheet; reprinted with permission from Ref. [78], Copyright © 2024, The Authors.

4.2. MOF-based MMMs

MMMs, by incorporating inorganic or inorganic/organic hybrid materials into a polymer matrix, overcome the poor membrane-forming ability of traditional inorganic materials and the disordered conducting pathways of polymer-based materials. In the field of proton-conducting membranes, MOFs show great potential as dispersed phases. However, their practical application still faces

two major challenges: (1) poor interfacial compatibility between MOFs and the polymer matrix, which easily leads to structural defects that hinder proton transport; (2) high MOF loading can cause particle aggregation and uneven membrane structures, thereby reducing proton conductivity. Therefore, enhancing interfacial interactions, improving MOF dispersion and increasing MOF loading are key aspects in the design of MMMs.

Fig. 6 summarizes several representative strategies for constructing high-performance MOF-based MMMs developed in recent years. In 2019, Liu and his co-workers [31] proposed a polymer-confinement encapsulation strategy, where poly(4-styrenesulfonate) (PSS) was precisely introduced into the three-dimensional(3D) pore network of ZIF-8 to fabricate a PSS@ZIF-8 membrane (Fig. 6a). This method established a continuous proton transport network and effectively addressed the interfacial incompatibility between MOFs and polymer matrices. The hybrid framework formed a dense hydrogen-bonding network between sulfonic acid groups and confined water molecules, enabling continuous proton-hopping pathways and achieving a high proton conductivity of 2.59×10^{-1} S cm^{-1} at 80 °C and 100% RH, surpassing most MOF-based conductors and even commercial Nafion membranes.

In 2020, Liu's group [77] further demonstrated a fiber-reinforced MMM fabricated via electrospinning. In this Ni-BDC/PAN system, 2D MOF nanosheets were aligned along polymer fibers to form 1D proton-conductive pathways (Fig. 6b). After vapor-phase loading of H_3PO_4 and imidazole, the resulting membranes exhibited proton conductivities of 1.05×10^{-2} and 6.04×10^{-5} S cm^{-1} at 80 °C and 90% RH, respectively, significantly improving the transport efficiency of the inorganic filler phase.

More recently, in 2023, Shimizu and co-workers [76] reported a PCMOF/CNC composite membrane with an exceptionally high MOF loading of 89 wt% (Fig. 6c). By leveraging hydrogen bonding interactions between cellulose nanocrystals (CNCs) and the layered PCMOF10 structure, they successfully enhanced interfacial proton transport while maintaining membrane integrity. Under 85 °C and 95% RH, this composite membrane delivered a proton conductivity of 1.44×10^{-2} S cm^{-1}, breaking through the long-standing limitation of low MOF content in traditional MMMs.

5. Application of proton-conducting MOF membranes

Proton-conducting MOF membranes have attracted growing attention owing to their well-defined porous architectures, tunable functional sites, and excellent chemical and thermal stability. These materials offer significant advantages over conventional polymers and inorganic proton conductors, particularly in terms of structural customizability and multifunctionality. Consequently, their application scope has extended beyond traditional proton exchange membranes (PEMs) to encompass proton sensors, photoelectronic devices, protonic diodes, and H^+-FETs. This section presents an overview of recent progress in MOF-based proton-conducting membranes for emerging device applications, highlighting their potential to enable next-generation protonic systems.

5.1. PEMs

As the core component of PEMFCs, PEMs serve to facilitate efficient proton transport while simultaneously preventing fuel and electron crossover. Although Nafion remains the industry benchmark, its limitations—such as poor performance at high temperature and low humidity conditions, high methanol permeability, and elevated production costs—have driven the search for

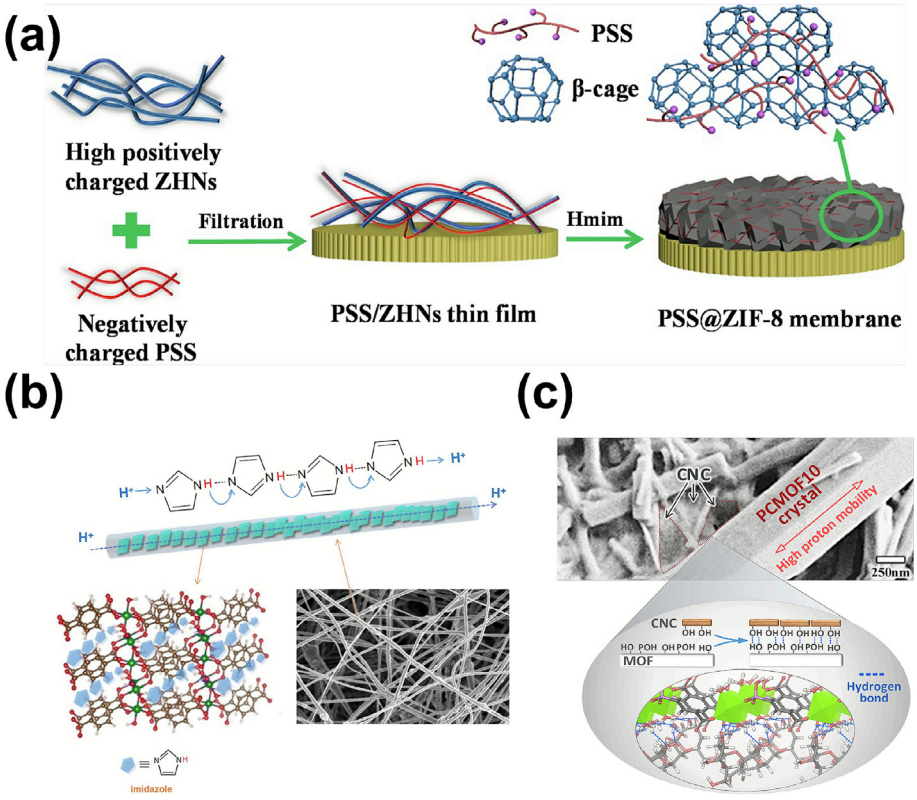

Fig. 6. Representative structures and fabrication strategies of MOF-based MMMs. (a) Schematic of precise polymer encapsulation within MOF pores to fabricate PSS@ZIF-8 mixed matrix membranes; reprinted with permission from Ref. [31], Copyright © 2019, Elsevier B.V. (b) One-dimensional nanofiber structure of Ni-BDC/PAN and its proton transport mechanism; reprinted with permission from Ref. [77], Copyright © 2020, IOP Publishing. (c) Ultrahigh MOF loading PCMOF/CNC membrane and schematic illustration of strong hydrogen bonding within the material; reprinted with permission from Ref. [76], Copyright © 2023, Elsevier B.V.

advanced alternatives with enhanced stability and tunable transport properties. MOF-based PEMs, especially in the form of MMMs, have shown considerable promise in addressing these issues. Their structural modularity allows for the integration of abundant proton-donating sites and robust thermal frameworks into flexible polymer matrices. These hybrid membranes exhibit improved water retention, directional transport pathways and mechanical strength.

To promote anhydrous proton conduction, Liu et al. [88] (2021) functionalized UiO-66 with phosphate-containing glyphosate ligand, introducing additional Brønsted acid sites. The modified MOF (1:2G-UiO-66) was incorpotated into a poly(4,4′-diphenyl ether-5,5′-bibenzimidazole) (OPBI) matrix to form a composite membrane. This hybrid system exhibited a high proton conductivity of 0.124 S cm^{-1} at 160 °C under dry conditions, and achieved a peak power density of 0.725 W cm^{-2}, significantly outperforming Nafion under comparable similar environments.

Zhao et al. [89] prepared a ZIF-67@Nafion composite membrane via the *in situ* growth of ZIF-67 nanoparticles on polyacrylonitrile nanofiber mats (PAN NFMs), followed by incorporation into the Nafion matrix (Fig. 7a). Strong hydrogen bonding between ZIF-67's amine groups and Nafion's sulfonic acid moieties facilitated

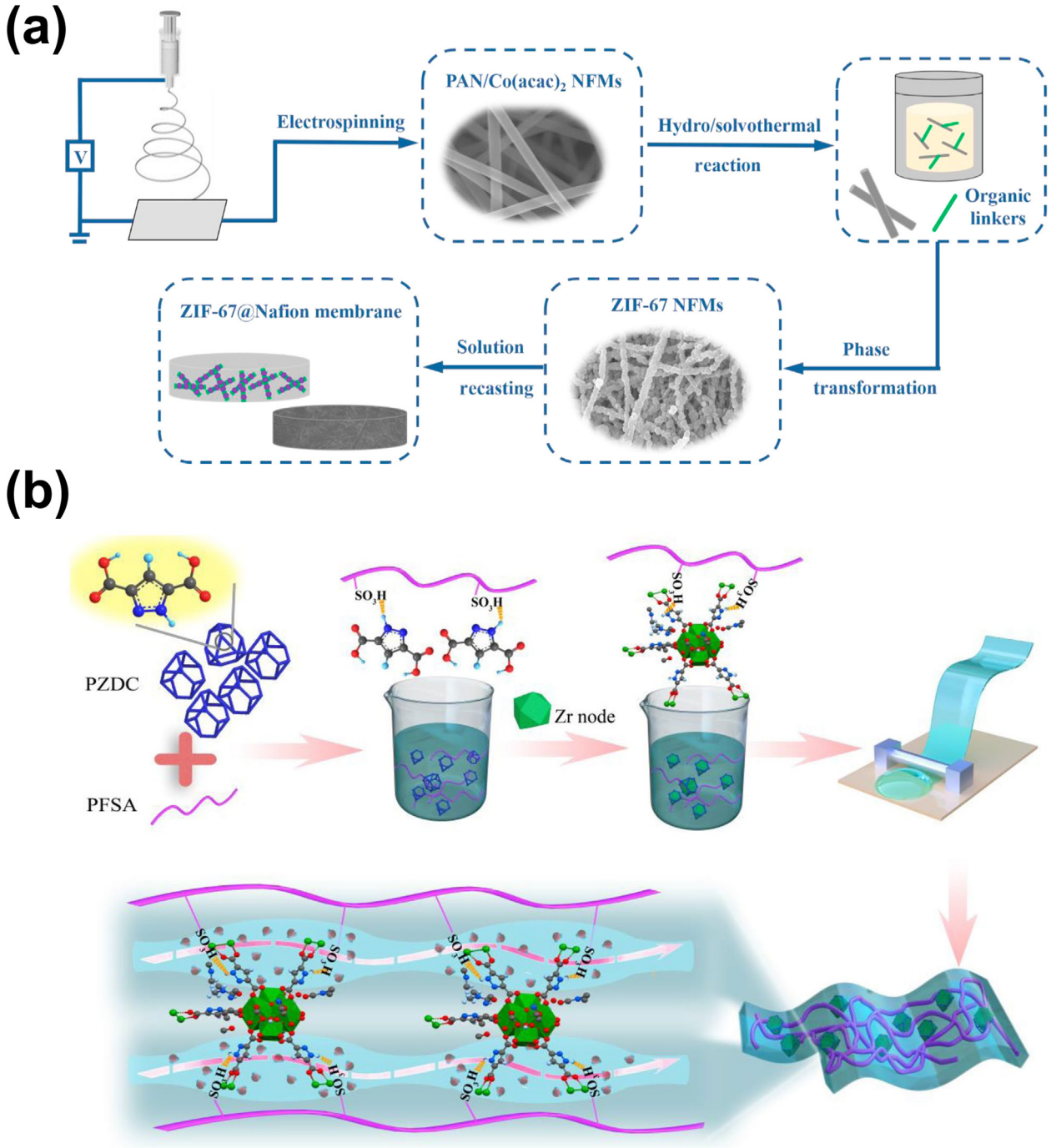

Fig. 7. Fabrication routes of ZIF-67 and NH-Zr MOF-based MMMs. (a) Fabrication routes of ZIF-67 NFMs and ZIF-67@Nafion composite membranes; reprinted with permission from Ref. [89], Copyright © 2021, Elsevier B.V. (b) Schematic illustration of NH-Zr MOF hybrid membrane preparation; reprinted with permission from Ref. [90], Copyright © 2023, Springer Nature.

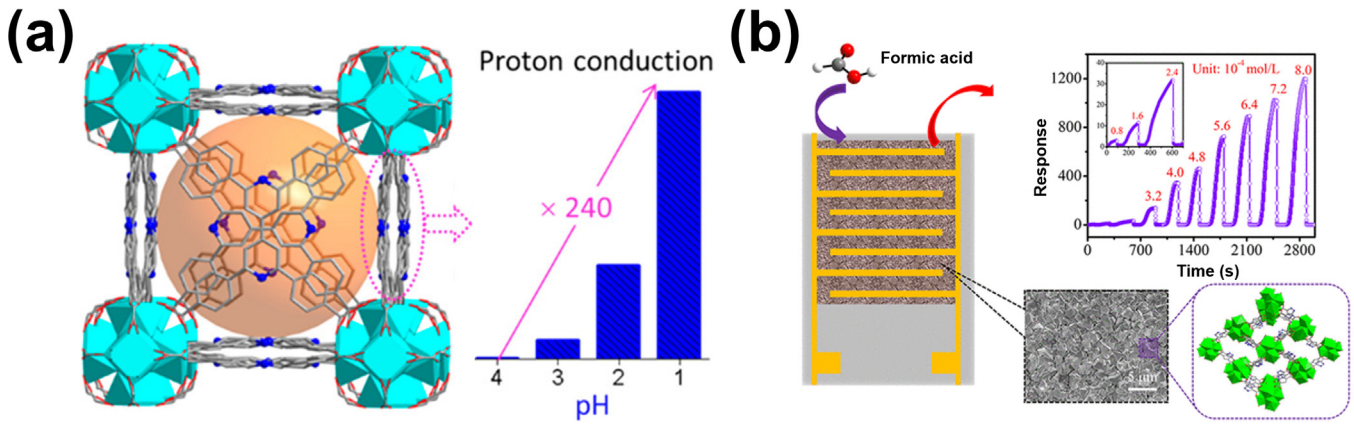

Fig. 8. Representative MOF-based proton sensors. (a) The pH responsiveness of zirconium-based MOFs; reprinted with permission from Ref. [35], Copyright © 2021, American Chemical Society. (b) Efficient formic acid detection using MOF-802 membrane device; reprinted with permission from Ref. [36], Copyright © 2021, American Chemical Society.

proton hopping via the Grotthuss mechanism. The resulting membrane demonstrated a proton conductivity of 0.288 S cm^{-1} and a peak power density of 0.298 W cm^{-2} at 80 °C and 100% RH. Additionally, methanol permeability was significantly reduced to 7.98 × 10^{-7} cm^2 s^{-1}, highlighting the selective barrier properties imparted by the MOF phase.

In 2023, Zhang et al. [90] constructed a composite membrane by embedding NH-functionalized Zr-MOFs into a perfluorosulfonic acid (PFSA) matrix (Fig. 7b). The -SO_3H groups on the MOF framework formed continuous hydrogen-bond networks, enhancing proton mobility under low-humidity conditions. Under 40% RH and 80 °C, the composite outperformed pristine PFSA by approximately 20% in proton conductivity, achieving a maximum power density of 0.726 W cm^{-2}.

Further enhancements in thermal stability were achieved by Xu et al. [91] (2024), who introduced Ce-BTC MOFs into PFSA membranes. Thermogravimetric analysis (TGA) confirmed improved thermal decomposition profiles. The resulting composite membranes exhibited continuously increasing proton conductivity with both temperature and MOF content, ultimately reaching a peak power density of 1.71 W cm^{-2} at 75 °C and 80% RH—substantially exceeding the performance of pristine Nafion. For practical operation in PEMFCs, proton-conducting MOF membranes must exhibit sufficient mechanical strength and dimensional stability to withstand hydration/dehydration cycles and external stresses encountered during device assembly and operation. In particular, membranes should possess tensile strengths of several megapascals and high resistance to cracking under humid conditions. These mechanical properties, along with recent advances in proton conductivity and interfacial engineering, will be crucial for translating MOF-based PEMs from laboratory prototypes to durable, device-level technologies.

5.2. Proton sensors

MOFs present unique advantages for proton sensing due to their structurally tunable pore environments that enable controlled proton transport, high surface area that facilitates efficient analyte interaction, and abundant functional sites that allow for proton-coupled recognition events. Their rigid frameworks and well-defined host-guest interactions enable sensitive and selective detection of changes in proton concentration, making them highly suitable for pH sensing and the recognition of specific protonic species. By incorporating specific functional groups (e.g., pyridyl, sulfonic acid, or carboxylate moieties), MOFs can respond to protonation events through measurable changes in conductivity, fluorescence, or optical absorption—offering a robust materials platform for next-generation proton sensors with high sensitivity and selectivity.

In 2021, Gao and co-workers [35] developed a zirconium-based MOF constructed from oxo-cluster nodes and bipyridyl-tetracarboxylate ligands that exhibited a strong fluorescence response to environmental pH variations (Fig. 8a). The sensing mechanism involved protonation of pyridyl groups, which induced a distinct redshift in the emission wavelength from 425 (blue) to 510 nm (green) as pH increased. The material also exhibited enhanced proton conductivity under acidic conditions, demonstrating dual-mode sensing via optical and electrical readouts. Beyond pH monitoring, the material showed potential for gaseous HCl gas detection, optical switching, and logic gate operation, highlighting the multifunctional potential of MOF-based proton sensors.

Ren's group [36] subsequently reported a thin-membrane chemical sensor based on MOF-802 for formic acid vapor detection at room temperature (RT) (Fig. 8b). The sensing mechanism relied on the formation of a hydrogen-bonding network between formic acid molecules and surface sites on the MOF membrane, producing highly selective and reproducible sensing signal outputs. The sensor exhibited excellent sensitivity due to the strong analyte-framework interactions. Furthermore, after four months of ambient storage, the response-recovery curves remained indistinguishable from the initial measurements, confirming the outstanding long-term stability and reliability of the MOF membrane sensor.

Building on this strategy, Ren's group [72] fabricated MOF-801 membrane via direct solvothermal growth on glass substrates. The resulting membranes were uniform and compact, enabling linear detection of formic acid over a broad concentration range (8.0 × 10^{-5} to 4.0 × 10^{-4} mol L^{-1}). The device exhibited a rapid response time (~100 s) and quick recovery to baseline upon analyte removal. Notably, repeated sensing cycles produced consistent signal intensities and response profiles, confirming the excellent operational stability and reversibility of the system. Over repeated cycling, the response-recovery curves remained virtually unchanged with negligible signal decay, underscoring the exceptional operational durability and repeatable performance of the MOF-801 membrane sensor.

5.3. Light-controlled protonic devices

Light-controlled protonic devices represent an emerging class of intelligent materials that regulate proton transport in response to optical stimuli. By incorporating photoresponsive units—such as

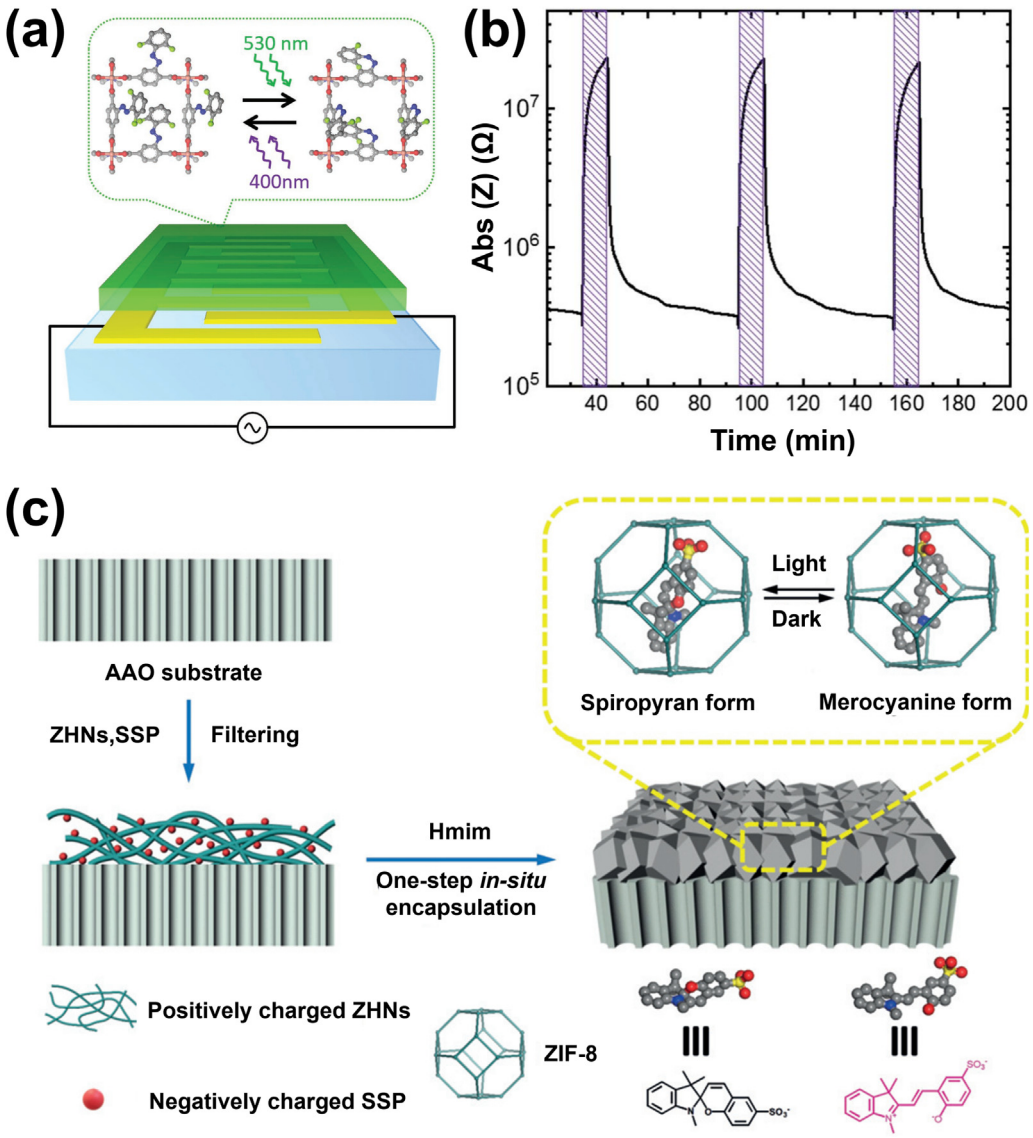

Fig. 9. Light-controlled MOF-based protonic devices. (a) Schematic structure of $Cu_2(F_2AzoBDC)_2(dabco)$ membrane with fluorinated azobenzene side groups; reprinted with permission from Ref. [73], Copyright © 2018, Wiley-VCH. (b) Time-dependent impedance magnitude (|Z|) of $Cu_2(SP\text{-}BPDC)_2(dabco)$ membrane at 1 Hz; reprinted with permission from Ref. [92], Copyright © 2020, The Royal Society of Chemistry. (c) Structure of SSP@ZIF-8 membrane and photoisomerization process of sulfonated spiropyran within the pores; reprinted with permission from Ref. [93], Copyright © 2020, Wiley-VCH.

azobenzene or spiropyran derivatives—into MOF frameworks, these systems undergo reversible isomerization under specific light wavelengths, thereby altering molecular dipoles, steric configurations, and hydrogen-bonding networks. These changes directly influence proton conduction pathways, enabling active modulation of conductivity through light exposure.

The use of thin-membrane configurations is particularly advantageous for such systems. Membranes enhance light penetration and minimize scattering, while also facilitating rapid and reversible structural transformations. Additionally, they offer improved mechanical stability, scalability, and integration into functional devices. As a result, the rational design of MOF-based photoresponsive membranes has become a key strategy for realizing programmable, light-switchable protonic systems.

In 2018, Heinke and his co-workers [73] reported the fabrication of a surface-anchored MOF (SURMOF) membrane, $Cu_2(F_2\text{-}AzoBDC)_2(dabco)$, incorporating fluorinated azobenzene side groups (Fig. 9a). Upon visible-light irradiation, the azobenzene moieties undergo *trans-cis* photoisomerization. X-ray diffraction confirmed the formation of highly oriented membranes. The *cis* configuration strengthened intramolecular hydrogen bonding, which restricted the mobility of proton carriers and thereby reduced proton conductivity from 1.2×10^{-6} to 7.9×10^{-7} S cm^{-1}. This light-induced switching process was fully reversible and could be repeated multiple times without degradation, demonstrating excellent photo-cycling stability. This study provided a clear proof-of-concept for optically gated proton transport using MOF membranes.

In 2020, Heinke's group [92] developed a spiropyran (SP)-based MOF membrane, $Cu_2(SP\text{-}BPDC)_2(dabco)$. Photoisomerization between the nonpolar SP and the polar merocyanine (MC) form significantly modulated proton conduction efficiency. In ethanol, the system showed a switching ratio of 20 (Fig. 9b), which increased to 82 in aqueous media and remained stable over repeated on/off cycles, demonstrating outstanding photoswitching durability. These results highlight the advantages of

spiropyran-functionalized frameworks over azobenzene-based analogs in amplifying photoinduced conductivity changes.

An alternative approach was reported by Fan et al. [93], who encapsulated sulfonated spiropyran (SSP) into the pores of ZIF-8 to create a hybrid membrane (SSP@ZIF-8) (Fig. 9c). This system achieved an ultrahigh switching ratio of 2.8×10^4 under 75 °C and 95% RH, with a fast response time of 5 s. Notably, this was the first demonstration of a light-triggered MOF protonic membrane operating in a functional device, successfully driving the on/off switching of a light-emitting diode (LED), thereby validating its potential for remote-controlled and optoelectronic applications. In 2021, they further expanded the concept by embedding the near-infrared photosensitizer indocyanine green (ICG) into the HSB-W5 framework to form a composite membrane (ICG@HSB-W5) [94]. Under dual-wavelength laser excitation (808 and 405 nm), the device exhibited reversible changes in proton conductivity and was able to perform basic molecular logic operations, including NOT, NAND, and NOR gates. A conductivity switching ratio of up to 1000 was achieved, marking the first integration of light-controlled proton conduction with logic functionality and paving the way for programmable MOF-based information processing systems.

5.4. H^+-FETs and proton rectifiers

H^+-FETs and proton rectifiers are pivotal components in emerging protonic electronics and energy-related technologies, such as proton-based logic circuits, fuel cells, and bioelectronic devices. These devices enable the precise regulation of proton transport under external electric fields or directional gradients. In protonic device architectures, MOFs stand out for their ability to combine efficient proton transport with structural adaptability, making them well-suited for high-performance H^+-FETs and rectifiers. Recent progress in this area has also accelerated the integration of MOF membranes into biointerfaces and molecular-scale electronics.

In 2019, Bodkhe et al. [32] introduced an imidazole-functionalization strategy to enhance the proton conductivity of Cu-BTC. The modified material, denoted Im@Cu-BTC, exhibited a proton conductivity of 1.04×10^{-4} S cm^{-1} at 70 °C and was integrated into an H^+-FET device. The resulting device showed clear field-effect behavior with bipolar transport characteristics, well-regulated drain current, a threshold voltage of ~7.0 V, and a stable ON/OFF current ratio, establishing MOFs as viable candidates for iontronic switching components.

In 2021, Xu and co-workers [33] developed an H^+-FET based on a highly ordered Cu-TCPP membrane (Fig. 10a), featuring 2D interstitial channels composed of alternating hydrophobic and hydrophilic domains. This structural configuration facilitated anisotropic proton migration under gate modulation. Electrical characterization revealed pronounced field-induced conductivity enhancement. Specifically, the gate voltage increased the proton concentration in the active layer from 0.9×10^{17} to 4.2×10^{17} cm^{-3} (Fig. 10b), accompanied by a proton mobility of 9.5×10^{-3} cm^2 (V s)$^{-1}$ and an ON/OFF ratio of 4.1. These metrics represent benchmark-level performance for MOF-based H^+-FETs, validating their potential in low-power protonic logic devices.

Kitagawa's group [85] reported in 2022 an all-solid-state proton rectifier constructed from a Cu_2(CuTCPP)/Mg-Al-LDH heterostructure (Fig. 10c). Individually, the Cu_2(CuTCPP) and LDH(NO_3) layers exhibited symmetric, linear current-voltage (*I-V*) responses. However, the heterojunction membrane displayed pronounced rectification behavior under 90% RH (Fig. 10d). When subjected to ±10 V alternating bias, the device achieved a rectification ratio exceeding 200 under forward bias, representing one of the highest values reported to date for MOF-based ionic rectifiers. The rectification effect arises from asymmetric proton transport across the junction interface, facilitated by differing electrochemical

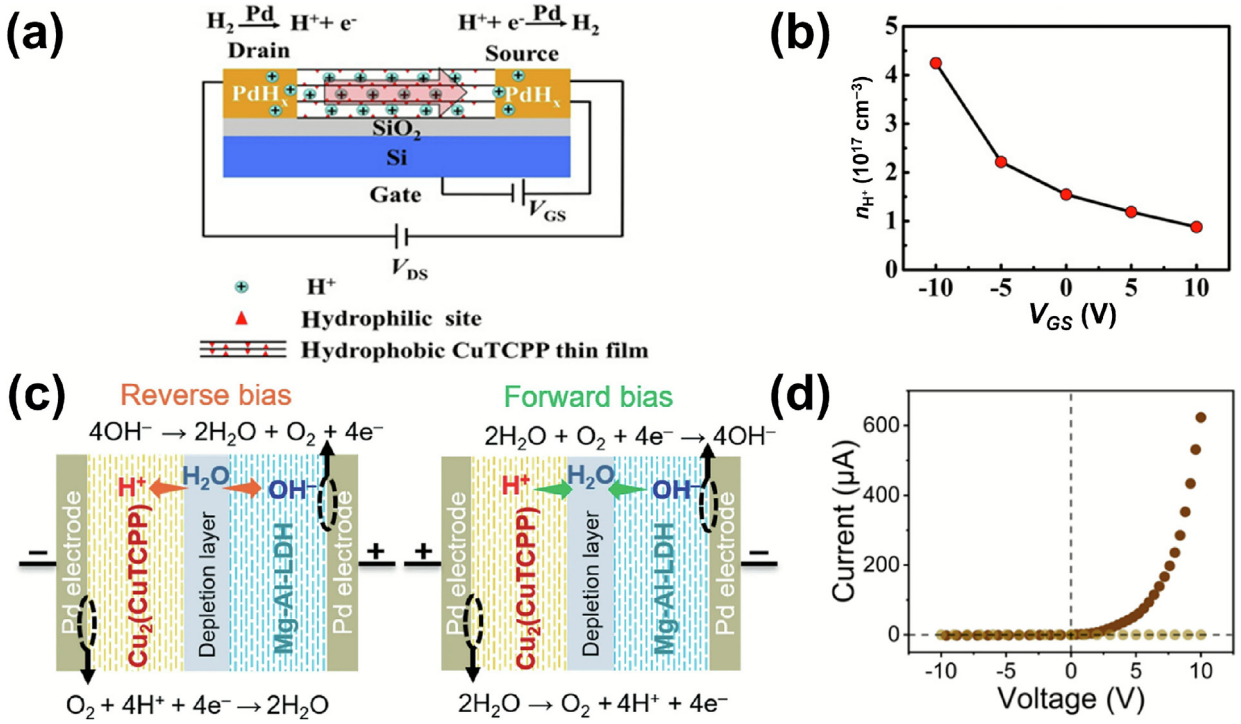

Fig. 10. Structural design and performance of MOF-based protonic H^+-FET and rectifier. (a) Structure and working principle of Cu-TCPP-based H^+-FET device. (b) Proton concentration in Cu-TCPP active layer under different voltages; reprinted with permission from Ref. [33], Copyright © 2021, Wiley-VCH. (c) Schematic of proton rectification mechanism in Cu_2(CuTCPP)/Mg-Al-LDH heterostructure rectifier. (d) *I-V* curves of the heterostructure under varying humidity conditions; reprinted with permission from Ref. [85], Copyright © 2022, Wiley-VCH.

Table 1
Summary of representative proton-conducting MOF membranes.

Compound	Fabrication method	Conductivity (S cm^{-1})	Mechanism (*Ea* (eV))	Condition
Cu-TCPP [49]	Modular assembly	3.9×10^{-3}	Grotthuss (0.28)	98% RH, 25 °C
HKUST-1 [83]	*In situ* growth	6.9×10^{-4}		98% RH, RT
NENU-3 [84]	Electrochemical deposition	1.4×10^{-5}	Grotthuss and vehicle (0.38)	97% RH, 24 °C
Cu_3TCPP [85]	Vacuum filtration	3.9×10^{-3}		98% RH, 25 °C
Cu-BDC [86]	Vacuum filtration	7.2×10^{-4}	Grotthuss and vehicle (0.38)	wet condition, 28 °C
Cu_2Ni-TCPP [87]	Vacuum filtration	1.3×10^{-5}	Grotthuss (0.2)	98% RH, 45 °C
a_gZW-MOF·HA [78]	Melt-quenching	1.57×10^{-2}		dry condition, 100 °C
PSS@ZIF-8 [31]	*In situ* growth	2.59×10^{-1}	vehicle (0.55)	100% RH, 80 °C
Ni-BDC/PAN [77]	Solution evaporating casting	1.05×10^{-2}	vehicle (0.82)	90% RH, 80 °C
PCMOF10/CNC [76]	Compression molding	1.44×10^{-2}	Grotthuss (0.33)	95% RH, 85 °C
UiO-66/OPBI [88]	Solution evaporating casting	1.24×10^{-1}		dry condition, 160 °C
ZIF-67@Nafion [89]	Solution evaporating casting	2.88×10^{-1}	Grotthuss (0.13)	100% RH, 80 °C
Zr-MOFs/PFSA [90]	Solution evaporating casting	2.92×10^{-1}	Grotthuss (0.2)	80% RH, 100 °C
Ce-BTC/PFSA [91]	Solution evaporating casting	1.95×10^{-1}	Grotthuss(0.16)	100% RH, 80 °C
Zr-TCPBP [35]	*In situ* growth	1.2×10^{-3}	Grotthuss (0.17)	98% RH, 68 °C
MOF-801 [72]	*In situ* growth	2.45×10^{-3}	Grotthuss (0.19)	98% RH, 75 °C
$Cu_2(F_2AzoBDC)_2$(dabco) [73]	Dip coating	1.2×10^{-4}		1,2,3-triazole-loaded, RT
Cu_2(SP-BPDC)$_2$(dabco) [92]	Dip coating	2.5×10^{-6}		93% RH, RT
SSP@ZIF-8 [93]	*In situ* growth	5×10^{-2}	Grotthuss and vehicle (0.43)	95% RH, 75 °C
ICG@HSB-W5 [94]	*In situ* growth	1.91×10^{-4}	vehicle (0.75)	95% RH, 55 °C

potentials and diffusion coefficients between the two layers. Overall, the representative proton-conducting MOF membranes covered in Sections 4 and 5 are comparatively summarized in Table 1, highlighting their fabrication methods, conduction mechanisms, and key performance metrics.

6. Conclusion and outlook

MOFs have emerged as a versatile and highly tunable class of materials for proton conduction, owing to their crystalline porous architectures, modular chemical composition, and extensive functionalization possibilities. By tailoring organic linkers, metal nodes, and guest species, researchers have achieved precise control over proton transport pathways, enabling both Grotthuss and vehicle mechanisms to be selectively modulated. Notably, the development of stimuli-responsive MOFs—capable of dynamically adjusting their conduction behavior in response to thermal, optical, electrical, or chemical inputs—has opened new avenues for the construction of programmable and adaptive protonic systems.

In the context of membrane technologies, the incorporation of MOFs into polymeric or composite matrices has proven effective in enhancing both proton conductivity and mechanical durability, particularly under challenging conditions such as high temperature and low humidity. MOF-based membranes and MMMs have shown substantial promise in surpassing the limitations of traditional PEMs, offering superior structural order, tunable interface chemistry, and multifunctionality. Despite notable progress, key challenges remain before large-scale deployment. These include long-term structural stability under variable humidity and temperature, integration with flexible or miniaturized device platforms, scalable membrane fabrication, and maintaining high conductivity under low-humidity or anhydrous conditions. Addressing these issues will be critical for translating laboratory-scale performance into practical technologies.

Looking forward, future research should prioritize the following directions: mechanistic understanding of MOF-polymer interactions to guide the rational design of high-performance MMMs with continuous proton conduction channels and minimized interfacial defects; in parallel, pure MOF membranes are expected to evolve toward ultrathin, ordered, functionalized, and stability-enhanced architectures to meet device-level requirements; advanced interface engineering between MOFs and ionic liquids or protic solvents to construct hybrid systems capable of stable, anhydrous proton transport; materials and device stability optimization under intermediate-to-high temperature conditions, including resistance to mechanical deformation and chemical degradation; computational modeling, defect engineering, and interface simulation are expected to accelerate the discovery and optimization of next-generation MOF membranes with controllable conduction pathways.

Continued progress in these areas is expected to accelerate the integration of MOF-based proton conductors into real-world applications such as fuel cells, flexible/wearable electronics, and intelligent sensing platforms. Ultimately, the convergence of MOF chemistry, device engineering, and responsive functionality will drive the evolution of next-generation protonic technologies toward higher efficiency, adaptability, and system-level integration.

Conflict of interest

The authors declare that they have no conflict of interest.

Acknowledgments

This work was supported by the National Natural Science Foundation of China (22405274, 22325109, 22171263, 62227815, 22494633, 22271281, 22422508, and 22505265), Self-deployment Project Research Program of Haixi Institutes, Chinese Academy of Sciences (CXZX-2023-GS03 and CXZX-2022-JQ03), China Postdoctoral Science Foundation (GZB20240748, 2023M743496, 2025M771085, and GZB20250273), the Key Research Project of Chinese Academy of Sciences under Grant (KGFZD-145-25-21), and Strategic Priority Research Program of the Chinese Academy of Sciences (XDB1170000).

Author contributions

Jiangfeng Lu and Yiming Xu conceived the overall framework of the review, performed the comprehensive literature survey, analyzed and synthesized the key advances, and prepared all figures, tables, and the initial manuscript draft. Yongjun Chen, Xiaoqing Yu, and Guane Wang assisted in collecting selected references and provided feedback on the manuscript structure. Hiroshi Kitagawa and Gang Xu supervised the project, provided strategic guidance, and offered critical revisions that shaped the final version of the manuscript.

References

[1] Yaghi OM, Li G, Li H. Selective binding and removal of guests in a microporous metal–organic framework. Nature 1995;378:703–6.
[2] Furukawa H, Cordova KE, O'Keeffe M, et al. The chemistry and applications of metal–organic frameworks. Science 2013;341:1230444.
[3] He T, Kong XJ, Li JR. Chemically stable metal–organic frameworks: rational construction and application expansion. Acc Chem Res 2021;54:3083–94.
[4] Kitagawa S, Kitaura R, Noro S. Functional porous coordination polymers. Angew Chem 2004;43:2334–75.
[5] Kitagawa S. Metal–organic frameworks (MOFs). Chem Soc Rev 2014;43:5415–8.
[6] Cai G, Yan P, Zhang L, et al. Metal–organic framework-based hierarchically porous materials: synthesis and applications. Chem Rev 2021;121:12278–326.
[7] Zhang Y, Liu H, Gao F, et al. Application of MOFs and COFs for photocatalysis in CO_2 reduction, H_2 generation, and environmental treatment. EnergyChem 2022;4:100078.
[8] Wang Q, Astruc D. State of the art and prospects in metal–organic framework (MOF)-based and MOF-derived nanocatalysis. Chem Rev 2019;120:1438–511.
[9] Ding M, Flaig RW, Jiang HL, et al. Carbon capture and conversion using metal–organic frameworks and MOF-based materials. Chem Soc Rev 2019;48:2783–828.
[10] Jiao L, Wang Y, Jiang HL, et al. Metal–organic frameworks as platforms for catalytic applications. Adv Mater 2018;30:1703663.
[11] Li YM, Yuan J, Ren H, et al. Fine-tuning the micro-environment to optimize the catalytic activity of enzymes immobilized in multivariate metal–organic frameworks. J Am Chem Soc 2021;143:15378–90.
[12] Jo YM, Jo YK, Lee JH, et al. MOF-based chemiresistive gas sensors: toward new functionalities. Adv Mater 2023;35:2206842.
[13] Shen Y, Tissot A, Serre C. Recent progress on MOF-based optical sensors for VOC sensing. Chem Sci 2022;13:13978–4007.
[14] Chen WH, Luo GF, Vázquez-González M, et al. Glucose-responsive metal–organic-framework nanoparticles act as "smart" sense-and-treat carriers. ACS Nano 2018;12:7538–45.
[15] Kreno LE, Leong K, Farha OK, et al. Metal–organic framework materials as chemical sensors. Chem Rev 2012;112:1105–25.
[16] Alezi D, Belmabkhout Y, Suyetin M, et al. MOF crystal chemistry paving the way to gas storage needs: aluminum-based soc-MOF for CH_4, O_2, and CO_2 storage. J Am Chem Soc 2015;137:13308–18.
[17] Daglar H, Gulbalkan HC, Avci G, et al. Effect of metal–organic framework (MOF) database selection on the assessment of gas storage and separation potentials of MOFs. Angew Chem 2021;60:7828–37.
[18] Fan W, Zhang X, Kang Z, et al. Isoreticular chemistry within metal–organic frameworks for gas storage and separation. Coord Chem Rev 2021;443:213968.
[19] Shi Z, Tao Y, Wu J, et al. Robust metal-triazolate frameworks for CO_2 capture from flue gas. J Am Chem Soc 2020;142:2750–4.
[20] Chen Z, Mian MR, Lee SJ, et al. Fine-tuning a robust metal–organic framework toward enhanced clean energy gas storage. J Am Chem Soc 2021;143:18838–43.
[21] Xu T, Jiang W, Tao Y, et al. Popping and locking: balanced rigidity and porosity of zeolitic imidazolate frameworks for high-productivity methane purification. J Am Chem Soc 2024;146:11225–34.
[22] Qian Q, Asinger PA, Lee MJ, et al. MOF-based membranes for gas separations. Chem Rev 2020;120:8161–266.
[23] Li S, Han W, An QF, et al. Defect engineering of MOF-based membrane for gas separation. Adv Funct Mater 2023;33:2303447.
[24] Li YZ, Wang GD, Ma LN, et al. Multiple functions of gas separation and vapor adsorption in a new MOF with open tubular channels. ACS Appl Mater Interfaces 2021;13:4102–9.
[25] Kitao T, Zhang Y, Kitagawa S, et al. Hybridization of MOFs and polymers. Chem Soc Rev 2017;46:3108–33.
[26] Iliescu A, Oppenheim JJ, Sun C, et al. Conceptual and practical aspects of metal–organic frameworks for solid-gas reactions. Chem Rev 2023;123:6197–232.
[27] Das A, Bej S, Pandit NR, et al. Recent advancements of metal–organic frameworks in sensing platforms: relevance in the welfare of the environment and the medical sciences with regard to cancer and SARS-CoV-2. J Mater Chem A 2023;11:6090–128.
[28] Liu YR, Chen YY, Zhuang Q, et al. Recent advances in MOFs-based proton exchange membranes. Coord Chem Rev 2022;471:214740.
[29] Kang DW, Kang M, Hong CS. Post-synthetic modification of porous materials: superprotonic conductivities and membrane applications in fuel cells. J Mater Chem A 2020;8:7474–94.
[30] Divya K, Liu Q, Murali R, et al. Integration of phosphorylated MOF/COF core-shell structures into hybrid membrane for high-temperature fuel cell application. Appl Surf Sci 2025;681:161544.
[31] Cai YY, Yang Q, Zhu ZY, et al. Achieving efficient proton conduction in a MOF-based proton exchange membrane through an encapsulation strategy. J Membr Sci 2019;590:117277.
[32] Bodkhe GA, Deshmukh MA, Patil HK, et al. Field effect transistor based on proton conductive metal–organic framework (Cu-BTC). J Phys D: Appl Phys 2019;52:335105.
[33] Wu GD, Zhou HL, Fu ZH, et al. MOF nanosheet reconstructed two-dimensional bionic nanochannel for protonic field-effect transistors. Angew Chem 2021;60:9931–5.
[34] Weber M, Kim JH, Lee JH, et al. High-performance nanowire hydrogen sensors by exploiting the synergistic effect of PD nanoparticles and metal–organic framework membranes. ACS Appl Mater Interfaces 2018;10:34765–73.
[35] Yang SL, Li G, Guo MY, et al. Positive cooperative protonation of a metal–organic framework: Ph-responsive fluorescence and proton conduction. J Am Chem Soc 2021;143:8838–48.
[36] Liu M, Zhang J, Kong YR, et al. Thin films of an ultrastable metal–organic framework for formic acid sensing with high selectivity and excellent reproducibility. ACS Mater Lett 2021;3:1746–51.
[37] Zhao Y, Wu M, Guo Y, et al. Metal–organic framework based membranes for selective separation of target ions. J Membr Sci 2021;634:119407.
[38] Deng T, Zeng X, Zhang C, et al. Constructing proton selective pathways using MOFs to enhance acid recovery efficiency of anion exchange membranes. Chem Eng J 2022;445:136752.
[39] Kanda S, Yamashita K, Ohkawa K. A proton conductive coordination polymer. I. [N, N'-bis(2-hydroxyethyl)-dithiooxamido] copper (II). Bull Chem Soc Jpn 1979;52:3296–301.
[40] Pal SC, Das MC. Superprotonic conductivity of MOFs and other crystalline platforms beyond 10^{-1} S cm^{-1}. Adv Funct Mater 2021;31:2101584.
[41] Kim S, Joarder B, Hurd JA, et al. Achieving superprotonic conduction in metal–organic frameworks through iterative design advances. J Am Chem Soc 2018;140:1077–82.
[42] Yang F, Xu G, Dou Y, et al. A flexible metal–organic framework with a high density of sulfonic acid sites for proton conduction. Nat Energy 2017;2:877–83.
[43] Joarder B, Lin JB, Romero Z, et al. Single crystal proton conduction study of a metal–organic framework of modest water stability. J Am Chem Soc 2017;139:7176–9.
[44] Wei YS, Hu XP, Han Z, et al. Unique proton dynamics in an efficient MOF-based proton conductor. J Am Chem Soc 2017;139:3505–12.
[45] Ramaswamy P, Wong NE, Shimizu GK. MOFs as proton conductors challenges and opportunities. Chem Soc Rev 2014;43:5913–32.
[46] Ye Y, Gong L, Xiang S, et al. Metal–organic frameworks as a versatile platform for proton conductors. Adv Mater 2020;32:1907090.
[47] Xue W, Sewell CD, Zhou Q, et al. Metal–organic frameworks for ion conduction. Angew Chem 2022;61:e202206512.
[48] Hermes S, Schröder F, Chelmowski R, et al. Selective nucleation and growth of metal–organic open framework thin films on patterned COOH/CF_3-terminated self-assembled monolayers on Au (111). J Am Chem Soc 2005;127:13744–5.
[49] Xu G, Otsubo K, Yamada T, et al. Superprotonic conductivity in a highly oriented crystalline metal–organic framework nanofilm. J Am Chem Soc 2013;135:7438–41.
[50] Shekhah O, Liu J, Fischer R, et al. MOF thin films: existing and future applications. Chem Soc Rev 2011;40:1081–106.
[51] Crivello C, Sevim S, Graniel O, et al. Advanced technologies for the fabrication of MOF thin films. Mater Horiz 2021;8:168–78.
[52] Agmon N. The grotthuss mechanism. Chem Phys Lett 1995;244:456–62.
[53] Kreuer KD, Rabenau A, Weppner W. Vehicle mechanism, a new model for the interpretation of the conductivity of fast proton conductors. Angew Chem 1982;21:208–9.

[54] Mukhopadhyay S, Debgupta J, Singh C, et al. Designing UiO-66-based superprotonic conductor with the highest metal–organic framework based proton conductivity. ACS Appl Mater Interfaces 2019;11:13423–32.
[55] Liu J, Zou X, Liu C, et al. Ionothermal synthesis and proton-conductive properties of NH_2-MIL-53 MOF nanomaterials. CrystEngComm 2016;18:525–8.
[56] Goesten MG, Juan Alcañiz J, Ramos Fernandez EV, et al. Sulfation of metal–organic frameworks: opportunities for acid catalysis and proton conductivity. J Catal 2011;281:177–87.
[57] Jeong NC, Samanta B, Lee CY, et al. Coordination-chemistry control of proton conductivity in the iconic metal–organic framework material HKUST-1. J Am Chem Soc 2012;134:51–4.
[58] Guo Y, Jiang Z, Ying W, et al. A DNA-threaded ZIF-8 membrane with high proton conductivity and low methanol permeability. Adv Mater 2018;30:1705155.
[59] Lim DW, Kitagawa H. Rational strategies for proton-conductive metal–organic frameworks. Chem Soc Rev 2021;50:6349–68.
[60] Shen D, Liu Y, Chen C, et al. Tuning electron cloud density in MOF nanosheets for enhanced proton conduction in PEMFCs. Adv Funct Mater 2025:e15358.
[61] Zhang Q, Zhang J, Qiu J, et al. Detecting the conduction property of proton carriers at different relative humidity based on postsynthetic MOF nanosheets. ACS Appl Mater Interfaces 2024;16:67697–705.
[62] Lazanas AC, Prodromidis MI. Electrochemical impedance spectroscopy—a tutorial. ACS Meas Sci Au 2023;3:162–93.
[63] Kolokolov DI, Lim DW, Kitagawa H. Characterization of proton dynamics for the understanding of conduction mechanism in proton conductive metal–organic frameworks. Chem Rec 2020;20:1297–313.
[64] Reif B, Ashbrook SE, Emsley L, et al. Solid-state NMR spectroscopy. Nat Rev Methods Primers 2021;1:2.
[65] Lim DW, Kitagawa H. Proton transport in metal–organic frameworks. Chem Rev 2020;120:8416–67.
[66] Phang WJ, Jo H, Lee WR, et al. Superprotonic conductivity of a UiO-66 framework functionalized with sulfonic acid groups by facile postsynthetic oxidation. Angew Chem 2015;54:5142–6.
[67] Liu SS, Han Z, Yang JS, et al. Sulfonic groups lined along channels of metal–organic frameworks (MOFs) for super-proton conductor. Inorg Chem 2019;59:396–402.
[68] Taylor JM, Dekura S, Ikeda R, et al. Defect control to enhance proton conductivity in a metal–organic framework. Chem Mater 2015;27:2286–9.
[69] Sadakiyo M, Yamada T, Kitagawa H. Rational designs for highly proton-conductive metal- organic frameworks. J Am Chem Soc 2009;131:9906–7.
[70] Rought P, Marsh C, Pili S, et al. Modulating proton diffusion and conductivity in metal–organic frameworks by incorporation of accessible free carboxylic acid groups. Chem Sci 2019;10:1492–9.
[71] Liu J, Wöll C. Surface-supported metal–organic framework thin films: fabrication methods, applications, and challenges. Chem Soc Rev 2017;46:5730–70.
[72] Lin FR, Liu ZY, Zhang H, et al. Proton conductive thin films of metal–organic framework for impedance detection of formic acid. Micropor Mesopor Mat 2023;360:112722.
[73] Muller K, Helfferich J, Zhao F, et al. Switching the proton conduction in nanoporous, crystalline materials by light. Adv Mater 2018;30:1706551.
[74] Babu AM, Varghese A. Electrochemical deposition for metal–organic frameworks: advanced energy, catalysis, sensing and separation applications. J Electroanal Chem 2023;937:117417.
[75] Li WJ, Liu J, Sun ZH, et al. Integration of metal–organic frameworks into an electrochemical dielectric thin film for electronic applications. Nat Commun 2016;7:11830.
[76] Lin S, Kedzior SA, Zhang J, et al. A superprotonic membrane derived from proton-conducting metal–organic frameworks and cellulose nanocrystals. Chem 2023;9:2547–60.
[77] Bai Z, Liu S, Chen P, et al. Enhanced proton conduction of imidazole localized in one-dimensional Ni-metal–organic framework nanofibers. Nanotechnology 2020;31:125702.
[78] Xue WL, Li GQ, Chen H, et al. Melt-quenched glass formation of a family of metal-carboxylate frameworks. Nat Commun 2024;15:2040.
[79] Ma N, Impeng S, Bureekaew S, et al. Photoexcited anhydrous proton conductivity in coordination polymer glass. J Am Chem Soc 2023;145:9808–14.
[80] Chen W, Horike S, Umeyama D, et al. Glass formation of a coordination polymer crystal for enhanced proton conductivity and material flexibility. Angew Chem 2016;55:5195–200.
[81] Chai M, Chen R, Xu K, et al. Ion transport and conduction in metal–organic framework glasses. J Mater Chem A 2023;11:20302–14.
[82] Xu G, Yamada T, Otsubo K, et al. Facile "modular assembly" for fast construction of a highly oriented crystalline MOF nanofilm. J Am Chem Soc 2012;134:16524–7.
[83] Qi Y, Lin S, Chen C, et al. Increased proton conductivity of metal–organic framework micro-film prepared by a facile salt-free approach. J Mater Chem A 2014;2:8849–53.
[84] Zhang F, Zhang T, Zou X, et al. Electrochemical synthesis of metal–organic framework films with proton conductive property. Solid State Ionics 2017;301:125–32.
[85] Lu J, Yoshida Y, Maesato M, et al. High-performance all-solid-state proton rectifier using a heterogeneous membrane composed of coordination polymer and layered double hydroxide. Angew Chem 2022;61:e202213077.
[86] Jing Y, Yoshida Y, Komatsu T, et al. A significant two-dimensional structural transformation in a coordination polymer that changes its electronic and protonic behavior. Angew Chem 2023;62:e202303778.
[87] Lu J, Yoshida Y, Kanamori K, et al. Robust proton conduction against mechanical stress in flexible free-standing membrane composed of two-dimensional coordination polymer. Angew Chem 2023;62:e202306942.
[88] Liu Y, Chen J, Fu X, et al. Constructing proton transport channels in low phosphoric-acid doped polybenzimidazole membrane by introducing metal–organic frameworks containing phosphoric-acid groups. J Power Sources 2021;507:230316.
[89] Zhao G, Shi L, Zhang M, et al. Self-assembly of metal–organic framework onto nanofibrous mats to enhance proton conductivity for proton exchange membrane. Int J Hydrogen Energy 2021;46:36415–23.
[90] Zhang W, Zhao S, Wang R, et al. Proton-conductive channels engineering of perfluorosulfonic acid membrane via *in situ* acid-base pair of metal–organic framework for fuel cells. Adv Compos Hybrid Mater 2023;6:60.
[91] Xu K, Liu G, Xu X, et al. Cerium based metal–organic framework as the efficient radical quencher for proton exchange membrane fuel cells. J Membr Sci 2024;699:122641.
[92] Kanj AB, Chandresh A, Gerwien A, et al. Proton-conduction photomodulation in spiropyran-functionalized MOFs with large on-off ratio. Chem Sci 2020;11:1404–10.
[93] Liang HQ, Guo Y, Shi Y, et al. A light-responsive metal–organic framework hybrid membrane with high on/off photoswitchable proton conductivity. Angew Chem 2020;59:7732–7.
[94] Fan S, Wang S, Wang X, et al. Optical-switched proton logic gate: indocyanine green decorated HSB-W5 MOFs nanosheets. Sci China Mater 2021;65:1076–86.